

# Research on Aerial Flyer Interception Based on Anti-aircraft Gun System

LIU HENG, MEI WEI, SHAN GAN LIN

Electronic and Optics Department  
Mechanical Engineering College  
Shijiazhuang, Hebei, 050000, China  
E-mail: oec\_lh86@163.com

*Abstract:* - In order to satisfy the requirements of anti-terrorism and security task, the interception methods of aerial flyer has been got much attention. According to the problem of low effectiveness-cost ratio of interception by missile traditionally, the feasibility of interception by anti-aircraft gun system is researched in the paper, two new interception methods, the point interception and barrage net interception are presented. The conception and idea of the two interception modes are proposed, and the maneuverability of the latter mode is validated by using probability theory. Finally, the validity of the two modes is verified through simulation. Results show that, point interception mode can be adopted when forecasting precision of aerial flyer is high, and barrage net mode can be used is applied in the condition of low forecasting precision, and the relationships between the two modes are not mutually exclusive and they are complementary.

*Key-Words:* - Anti-aircraft gun system; Point interception; Barrage net interception; Probability Theory; research

## 1 Introduction

Now with the diversification of anti-terrorism and security status, it is important to defend against aerial threat for important concourses such as conference building and important venues. Especially, in the recent Olympic Games, aerial defense missile has been disposed around the important Olympic venues [1], for instance, Patriot missile for the 2004 Athens Olympic Games and Small Sword-2000 for the 2012 London Olympic Games. But the military aerial defense missile system is not suitable in the defense task mentioned above. Firstly, usually the aerial threat targets are some small flyer with low altitude and slow velocity, for example, the helicopter model. But the missile is usually designed to intercept combat airplane. Secondly, the military aerial defense missile is costly, so when we adopt the missile, the effectiveness-cost ratio will be low. The last but not the least, the big volume of missile system equipment will affect its disposing quantity. By contrast, the anti-aircraft gun system is cheap and its volume is small, and then it could be dispersedly

disposed at an easy rate, which can improve its viability [2,3],consequently this system could effectively protect the security area. It is obvious that anti-aircraft gun system plays an irreplaceable role in terminal interception [4,5].

In the paper, we study the feasibility of aerial flyer interception around security area by anti-aircraft gun system. The conceptions and principle of the two interception modes are given out in Section2, and in Section3, maneuverability of the latter mode is proved by using probability theory. In Section 4, the validity of the two modes is verified through simulation and related applications are analyzed, Section 5, the conclusion are obtained.

## 2 Conception and Principle of Point interception and Barrage net interception mode

In the Fig. 1,  $O$  is origin of the coordinate,  $L$  is target flight path,  $l$  is its projection on the horizontal plane, the coordinate components of target present point  $M$  is  $(\beta, \varepsilon, D)$  or  $(X, Y, H)$ ,

$m$  is its projection on the horizontal plane,  $M_q$  is ahead point with coordinate components  $(\beta_q, \varepsilon_q, D_q)$  or  $(X_q, Y_q, H_q)$ . Basic vector equation for encountering calculation problem under standard shooting condition can be written as follows (1):

$$\begin{cases} \overline{D}_q = \overline{D} + \overline{S} \\ t_f = f(\overline{D}_q) \end{cases} \quad (1)$$

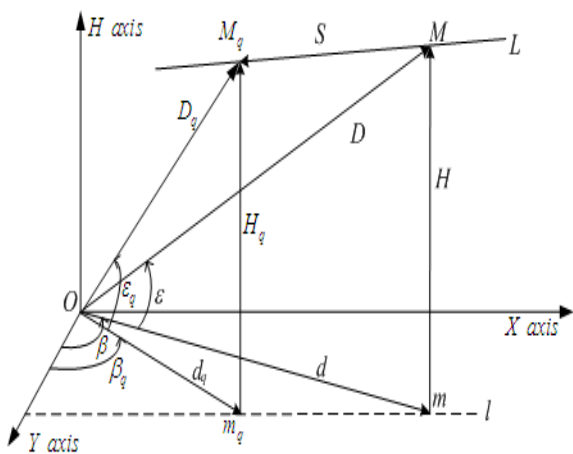


Fig 1. Principle drawing of shooting target

Where  $\overline{D}$  denotes present point vector,  $\overline{D}_q$  denotes ahead inclined distance vector,  $\overline{S}$  denotes position advances of target move,  $t_f$  denotes pill flight time during the process of encountering calculation.

Definition 1: take the target forecasting ahead point  $M_q$  as aiming point (named pill distribution center as well) of shooting data for each anti-aircraft gun in this system, and pills will obey Gaussian distribution and which center is on  $M_q$ , this mode is called Point interception.

Definition 2: each aiming point  $M_q^i$  is equably circular distribution with radius of  $r_j (j \geq 1)$  and centers are on ahead point  $M_q$  (named pill configuration center as well), and pills present the uniform distribution approximately and will be complanate in the point of  $M_q$  point, this mode is called barrage net interception.

As it can be found that, in the Fig. 2, the sketch map of each aiming point presents equably distributing on n circles. The mathematic principle of barrage net interception is described as follows: configure several pill centers with dispersed distribution, which obey Gaussian distribution, and if we apply its tail additive effect, and then an approximately well-proportioned pill distribution area is obtained. Fig.3 is the sketch map of one-dimensional approximately uniform distribution with three components of Gaussian tail additive effect.

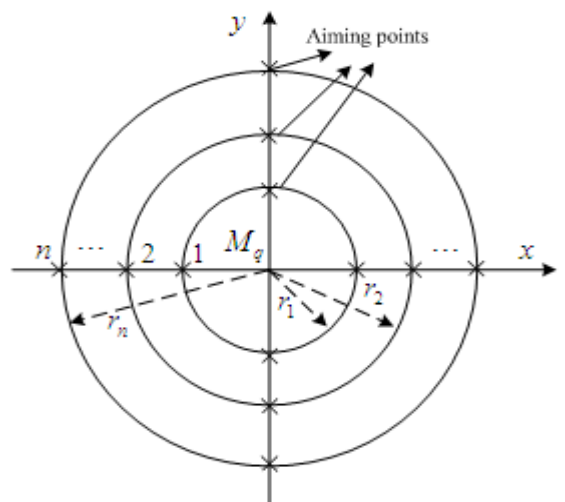


Fig 2. Sketch map of barrage net mode

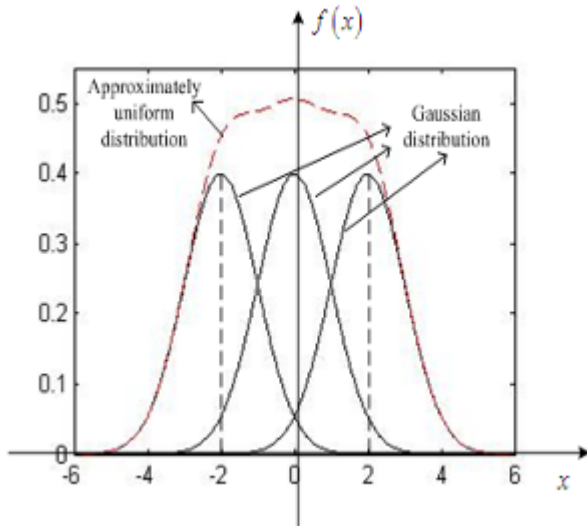


Fig 3. Uniform distribution and Gaussian distribution

### 3 Circular barrage net formed by pills that obey random Gaussian distribution

Theorem 1: Given that the forecasting plane in which target and pill will encounter introduced in paper[4] includes  $\sum_{i=1}^m n_i$  distribution centers  $\overline{X}_{i,l}$  that well-proportioned configuration along

$\|X\| = r_i$ , pills on the distribution circle  $i$  obey independent two-dimensional Gaussian distribution whose Mean Square Error (MSE) is  $\sigma_i^x = \sigma_i^y = \sigma_i$  as shown in Fig.2,

$$\overline{X}_{i,l} = \left( \overline{x}_{i,l} \quad \overline{y}_{i,l} \right)^T = \left( r_i \cos \frac{2\pi}{n_i} l \quad r_i \sin \frac{2\pi}{n_i} l \right)^T,$$

where  $i = 1, 2, \dots, m$ ,  $m$  is the number of distribution circles,  $l = 1, 2, \dots, n_i$ ,  $n_i$  is the number of distribution centers and  $r_i$  is radius of circle  $i$ .

Supposed that pill for each  $\overline{X}_{i,l}$  is equal, a circular barrage net will be formed when  $n_i \geq 3, r_i = \sqrt{2}\sigma_i$ , the integrated pill distribution density is planar on the configuration center  $M_q$ .

Based on theorem supposing, integrated pill distribution density can be described as

$$f(x, y) = \frac{1}{\sum_{i=1}^m n_i} \sum_{i=1}^m \sum_{l=1}^{n_i} \frac{1}{2\pi\sigma_i^2} \exp \left[ -\frac{1}{2\sigma_i^2} \left( \left( x - r_i \cos \frac{2\pi}{n_i} l \right)^2 + \left( y - r_i \sin \frac{2\pi}{n_i} l \right)^2 \right) \right] \quad (2)$$

$$k_p(0,0) = \frac{\partial^2 f(0,0)}{\partial p^2} = \left[ \frac{\partial^2 f(0,0)}{\partial x^2} \quad \frac{\partial^2 f(0,0)}{\partial x \partial y} \quad \frac{\partial^2 f(0,0)}{\partial y \partial x} \quad \frac{\partial^2 f(0,0)}{\partial y^2} \right] \quad (3)$$

= 0

If Eq.(3) comes true or does exists, and then  $f(x, y)$  is planar in point  $(0,0)$  [5-7].

Through the partial derivative calculating of Eq. (2), we can obtain the following equations.

$$\frac{\partial f(x, y)}{\partial x} = \sum_{i=1}^m \left\{ \frac{1}{2\pi\sigma_i^2 \sum_{i=1}^m n_i} \sum_{l=1}^{n_i} \frac{-\left( x - r_i \cos \frac{2\pi}{n_i} l \right)}{\sigma_i^2} \exp \left\{ -\frac{1}{2\sigma_i^2} \left[ \left( x - r_i \cos \frac{2\pi}{n_i} l \right)^2 + \left( y - r_i \sin \frac{2\pi}{n_i} l \right)^2 \right] \right\} \right\} \quad (4)$$

$$\frac{\partial f(x, y)}{\partial y} = \sum_{i=1}^m \left( \frac{1}{2\pi\sigma_i^2 \sum_{l=1}^{n_i} n_i} \frac{-\left(y - r_i \sin \frac{2\pi l}{n_i}\right)}{\sigma_i^2} \exp \left\{ -\frac{1}{2\sigma_i^2} \left[ \left(x - r_i \cos \frac{2\pi l}{n_i}\right)^2 + \left(y - r_i \sin \frac{2\pi l}{n_i}\right)^2 \right] \right\} \right) \quad (5)$$

$$\frac{\partial^2 f(x, y)}{\partial x^2} = \sum_{i=1}^m \left( \frac{1}{2\pi\sigma_i^2 \sum_{l=1}^{n_i} n_i} \frac{\left(x - r_i \cos \frac{2\pi l}{n_i}\right)^2 - \sigma_i^2}{\sigma_i^4} \exp \left\{ -\frac{1}{2\sigma_i^2} \left[ \left(x - r_i \cos \frac{2\pi l}{n_i}\right)^2 + \left(y - r_i \sin \frac{2\pi l}{n_i}\right)^2 \right] \right\} \right) \quad (6)$$

$$\frac{\partial^2 f(x, y)}{\partial y^2} = \sum_{i=1}^m \left( \frac{1}{2\pi\sigma_i^2 \sum_{l=1}^{n_i} n_i} \frac{\left(y - r_i \sin \frac{2\pi l}{n_i}\right)^2 - \sigma_i^2}{\sigma_i^4} \exp \left\{ -\frac{1}{2\sigma_i^2} \left[ \left(x - r_i \cos \frac{2\pi l}{n_i}\right)^2 + \left(y - r_i \sin \frac{2\pi l}{n_i}\right)^2 \right] \right\} \right) \quad (7)$$

$$\frac{\partial^2 f(x, y)}{\partial x \partial y} = \sum_{i=1}^m \left( \frac{1}{2\pi\sigma_i^2 \sum_{l=1}^{n_i} n_i} \frac{\left(x - r_i \cos \frac{2\pi l}{n_i}\right) \left(y - r_i \sin \frac{2\pi l}{n_i}\right)}{\sigma_i^4} \exp \left\{ -\frac{1}{2\sigma_i^2} \left[ \left(x - r_i \cos \frac{2\pi l}{n_i}\right)^2 + \left(y - r_i \sin \frac{2\pi l}{n_i}\right)^2 \right] \right\} \right) \quad (8)$$

$$\frac{\partial^2 f(x, y)}{\partial y \partial x} = \frac{\partial^2 f(x, y)}{\partial x \partial y} \quad (9)$$

$$f' = \cos\left(\frac{4\pi}{3}\right) + \cos\left(\frac{8\pi}{3}\right) + \cos\left(\frac{12\pi}{3}\right) = 0 \quad (11)$$

When  $r_i = \sqrt{2}\sigma_i$ , using  $\cos^2(x) = \frac{1 + \cos(2x)}{2}$  in the simplifying of Eq. (6).

$$\frac{\partial^2 f(0, 0)}{\partial x^2} = \sum_{i=1}^m \left( \frac{\exp(-1)}{2\pi\sigma_i^4 \sum_{l=1}^{n_i} n_i} \sum_{l=1}^{n_i} \cos\left(\frac{4\pi l}{n_i}\right) \right) \quad (10)$$

Define  $f' = \sum_{l=1}^{n_i} \cos\left(\frac{4\pi l}{n_i}\right)$

When  $n_i = 3$ ,

When  $n_i = 4$ ,

$$f' = \cos\left(\frac{4\pi}{4}\right) + \cos\left(\frac{8\pi}{4}\right) + \cos\left(\frac{12\pi}{4}\right) + \cos\left(\frac{16\pi}{4}\right) = 0 \quad (12)$$

When  $n_i > 4$ , because  $\sin\left(\frac{4\pi}{n_i}\right) \neq 0$  and on the basis of

$$\sin(x) - \sin(y) = 2 \cos\left(\frac{x+y}{2}\right) \sin\left(\frac{x-y}{2}\right).$$

$$\begin{aligned}
 f' &= \csc\left(\frac{4\pi}{n_i}\right) \sum_{l=1}^{n_i} \cos\left(\frac{4\pi l}{n_i}\right) \sin\left(\frac{4\pi}{n_i}\right) = \frac{1}{2} \csc\left(\frac{4\pi}{n_i}\right) \sum_{l=1}^{n_i} \left[ \sin\frac{4(l+1)\pi}{n_i} - \sin\frac{4(l-1)\pi}{n_i} \right] \\
 &= \frac{1}{2} \csc\left(\frac{4\pi}{n_i}\right) \left( \sin\frac{4(n_i+1)\pi}{n_i} + \sin\frac{4n_i\pi}{n_i} - \sin\frac{4(1-1)\pi}{n_i} - \sin\frac{4\pi}{n_i} \right) = 0
 \end{aligned}$$

(13)

Therefore, on the basis of Eqs. (11)~(13), when  $n_i \geq 3, r_i = \sqrt{2}\sigma_i, \frac{\partial^2 f(0,0)}{\partial x^2} = 0$

In the same way, through related calculation that  $\frac{\partial^2 f(0,0)}{\partial y^2} = -\frac{\partial^2 f(0,0)}{\partial x^2} = 0,$

$$\frac{\partial^2 f(0,0)}{\partial x \partial y} = \frac{\partial^2 f(0,0)}{\partial y \partial x} = 0.$$

when  $n_i \geq 3, r_i = \sqrt{2}\sigma_i$ . Consequently, Eq.(3) comes

into existence. Here,  $f(0,0) = \sum_{i=1}^m \frac{n_i}{2\pi e|\sigma_i^2|}$ , an

circular barrage net is established, whose center is target forecasting ahead point  $M_q$ .

### 4 Simulation and analysis

Simulation part one: through theorem 1, we can assure that probability density is planar around target forecasting ahead point  $M_q$ . Now, the characteristics of pill distribution probability density function are analyzed under different parameters through simulation.

Simulation parameters are set as follows:

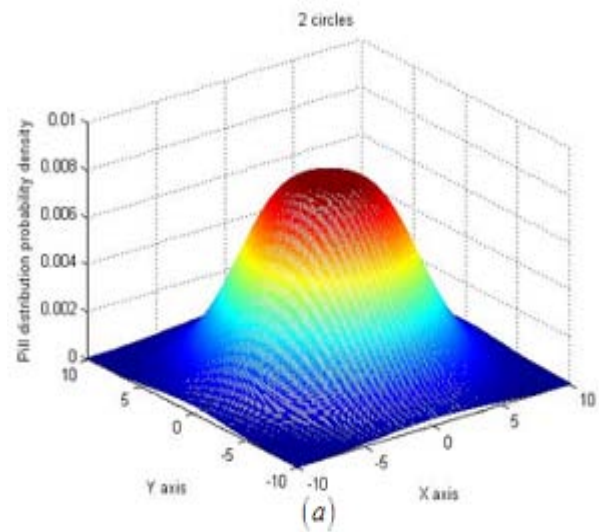
(1)  $m = 2, n_1 = n_2 = 6, r_1 = 2\sqrt{3}, r_2 = 3\sqrt{2}, \sigma_1 = \sqrt{6}, \sigma_2 = 3$

(2)  $m = 2, n_1 = n_2 = 6, r_1 = 2\sqrt{3}, r_2 = 3\sqrt{2}, \sigma_1 = \sqrt{3}, \sigma_2 = \sqrt{6}$

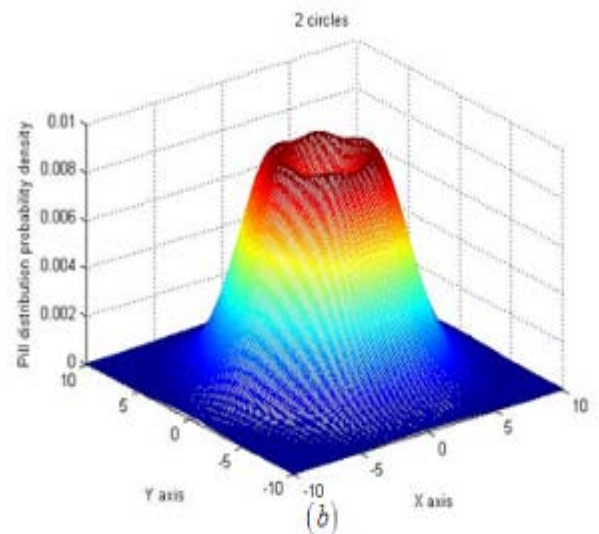
(3)  $m = 3, n_1 = n_2 = n_3 = 6, r_1 = 2\sqrt{3}, r_2 = 3\sqrt{2}, r_3 = 4\sqrt{2}, \sigma_1 = \sqrt{6}, \sigma_2 = 3, \sigma_3 = 4$

In the Fig.4, it gives out the pill distribution probability density function curve. Where, (a) of the

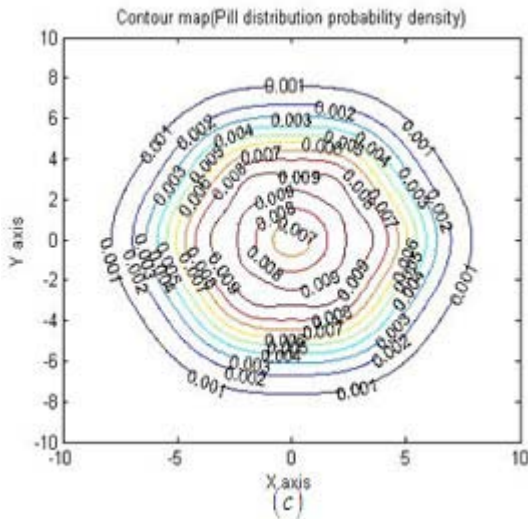
Fig.4 is three-dimensional mesh diagram of pill distribution probability density which according to with simulation parameters ( 1 ); (b) and (d) of the Fig.4 are corresponding with simulation parameters ( 2 ) and ( 3 ) respectively; (c) of the Fig.4 is contour map with label of (b).



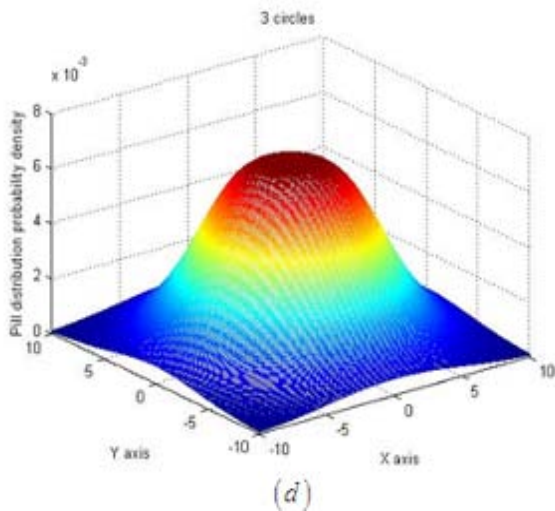
(a) Mesh diagram of pill distribution probability density corresponding with Simulation setup (1)



(b) Mesh diagram of pill distribution probability density corresponding with Simulation setup (2)



(c) Contour map of pill distribution probability density corresponding with Simulation setup (2)



(d) Mesh diagram of pill distribution probability density corresponding with Simulation setup (3)

Fig 4. Pill distribution probability density

In the (a) and (d) of Fig.4, it shows that when  $n_i \geq 3, r_i = \sqrt{2}\sigma_i$ , the pill distribution probability density is planar around point (0,0); As shown in (b) of Fig.4, Simulation setup is  $r_i \neq \sqrt{2}\sigma_i$  results in its inequality, and its value is less than that of around it, (c) of Fig.4 shows this variation disciplinary is more obviously. These results prove that theorem 1 is true.

Simulation part two: Efficiency of point interception and barrage net interception modes are compared and each application fields are analyzed.

Here, taking the number six distribution centers of barrage net circle as an example, namely that  $m=1, n=6$ . Given that the projection area of aerial flyer is a circle with acreage  $s=1 m^2$  in the forecasting plane,  $w=3$  denotes the required average number of pills hitting the target,  $f$  denotes pill distribution density function. If number of launching pills to target is  $N$ , then the intercept probability can be calculated by the equation (14) [8].

$$P_s(N) = 1 - [1 - (f \cdot s / w)]^N \quad (14)$$

Simulation setups

(1) Point interception:  $\sigma = \sqrt{2}$ , barrage net interception:  $r = 2, \sigma = \sqrt{2}, N = 50$

(2) Point interception:  $\sigma = \sqrt{2}$ , barrage net interception:  $r = 2, \sigma = \sqrt{2}, N = 200$

(3) Point interception:  $\sigma = \sqrt{2}$ , barrage net interception:  $r = \sqrt{6}, \sigma = \sqrt{3}, N = 200$

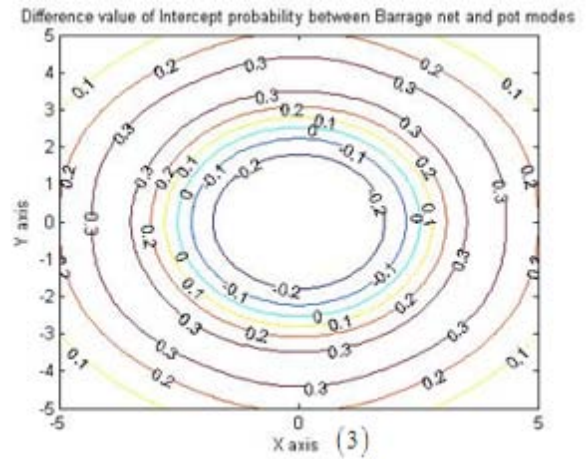
(4) Point interception:  $\sigma = \sqrt{2}$ , barrage net interception:  $r = \sqrt{2}, r = 2, r = \sqrt{6}, \sigma = r/\sqrt{2}, N = 200$

(5) Point interception:  $\sigma = \sqrt{2}$ , barrage net interception:

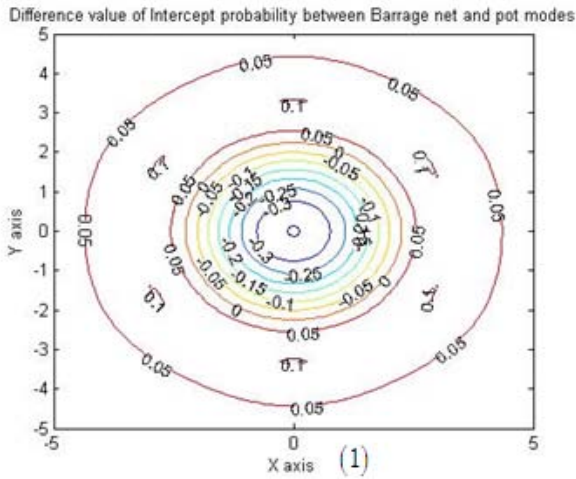
$$r = 2, \sigma = \sqrt{2}, N = 100, N = 200, N = 300$$

Fig. 5, Fig.6 and Fig.7 are the simulation results. Fig. 5 denotes difference value of intercept probability between barrage net and point interception mode under the same condition, where (1) and (4) correspond with simulation setup (1), here (1) is the map of camber contour, (4) is the figure of three-dimensional caber. In the same way, (2) and (5) correspond with simulation setup (2), (3) and (6) correspond with simulation setup (3); Fig. 6 denotes the pill distribution probability of the two interception modes under interception area of the same acreage, here, the area is expressed by radius  $rr_i = 0.5 * i, (i = 1, 2, \dots, 12)$ , this result corresponds with simulation setup (4), where, (a) denotes pill distribution probability under the circular area composed by the points which satisfy the condition of  $0 < r_d \leq rr_i, (i = 1, 2, \dots, 12)$ , here

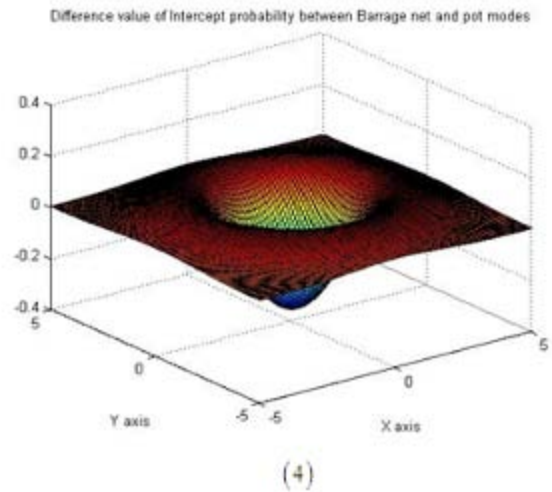
$r_d$  is the distance between the point and center of the circle. (b) denotes pill distribution probability under the looped area composed by the points which satisfy the condition of  $rr_i = 0.5 * i, rr_i < r_d^i \leq rr_{i+1} (i = 1, 2, \dots, 11)$ . (c) is the figure of two-dimensional vertical bar chart; Fig.7 denotes the interception area acreage of the two modes of whose intercept probability is greater than a certain lower limit value, this result corresponds with simulation setup (5).



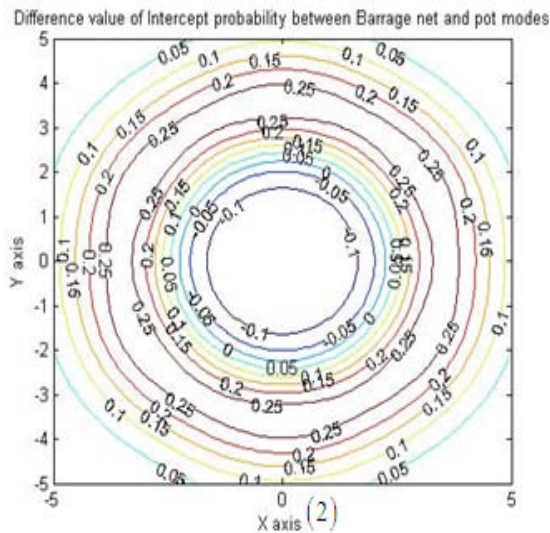
(3) Camber contour of difference value of intercept probability between Barrage net and Pot modes correspond with Simulation setup (3)



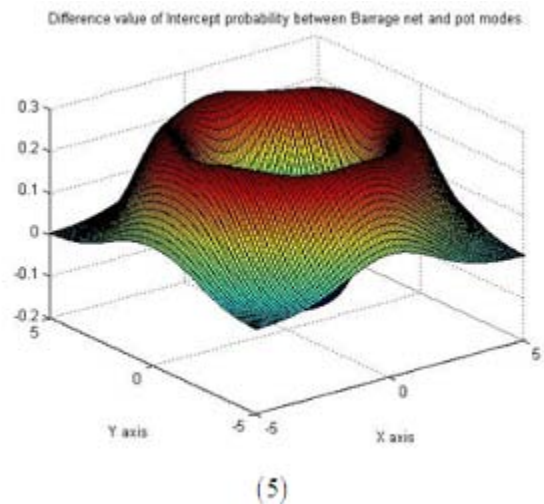
(1) Camber contour of difference value of intercept probability between Barrage net and Pot modes correspond with Simulation setup (1)



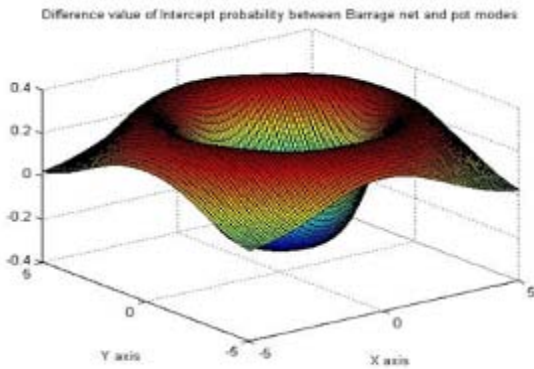
(4) Three-dimensional camber of difference value of intercept probability between Barrage net and Pot modes correspond with Simulation setup (1)



(2) Camber contour of difference value of intercept probability between Barrage net and Pot modes correspond with Simulation setup (2)



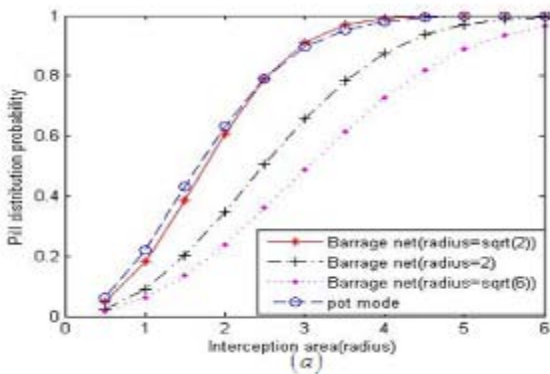
(5) Three-dimensional caber of difference value of intercept probability between Barrage net and Pot modes correspond with Simulation setup (2)



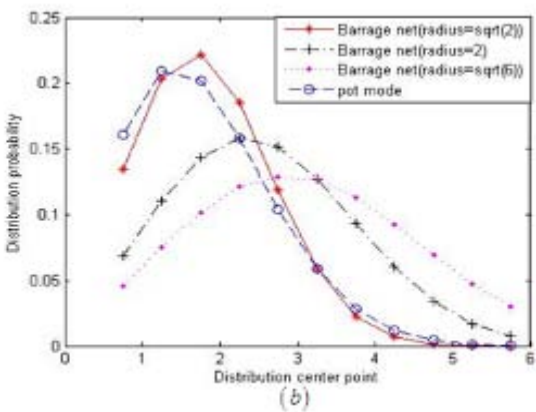
(6)

(6) Three-dimensional caber of difference value of intercept probability between Barrage net and Pot modes correspond with Simulation setup (3)

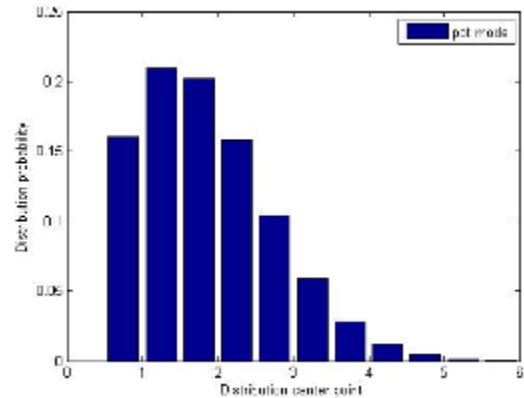
Fig 5. Different values of intercept probability for the two modes



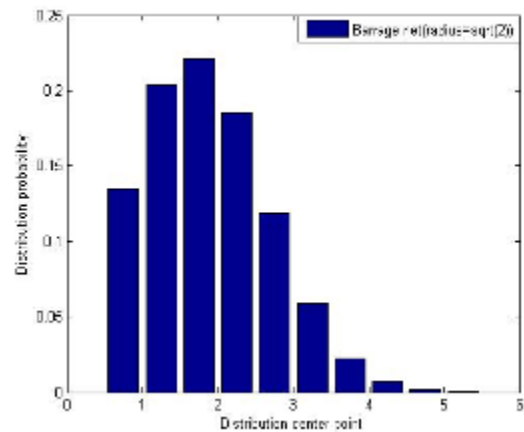
(a) Pill distribution probability under same circular area



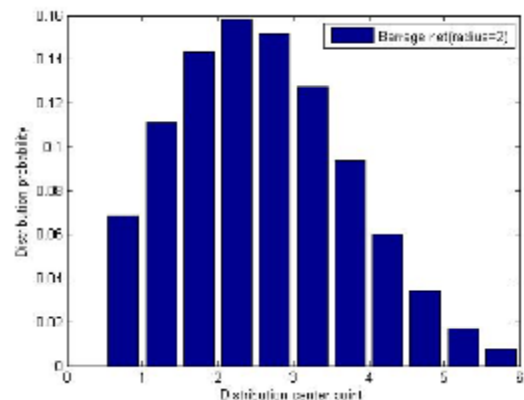
(b) Pill distribution probability under same looped area



(c-1) Figure of two-dimensional vertical bar chart for pot mode

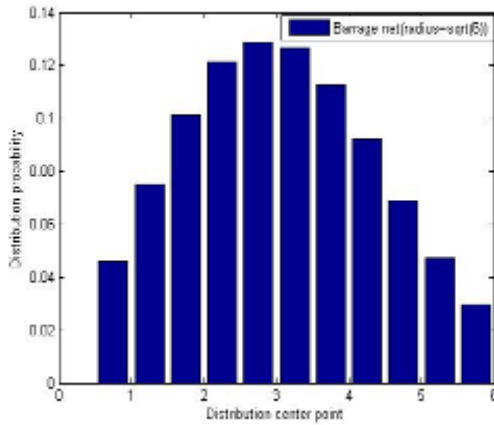


(c-2) Figure of two-dimensional vertical bar chart for barage net mode with radius =  $\sqrt{2}$



(c-3) Figure of two-dimensional vertical bar chart for barage net mode with radius = 2





(c-4) Figure of two-dimensional vertical bar chart for barrage net mode with radius =  $\sqrt{6}$

Fig 6. RelationshipS between pill distribution probability and interception area

Comparing Fig. 5-(1) with Fig. 5-(2), when pill number is few, efficiency of point interception is greater than that of barrage net interception on the whole, the latter is better than the former only in periphery, but here the intercept probability of both modes is not big enough to intercept target; however, when pill number is increased to 200, efficiency of barrage net interception is improved obviously, mostly in the two aspects: the first is that around pill configuration center, although point interception has little greater efficiency, but the intercept probability of barrage net is also big enough; the second is that barrage net mode has much more obvious advantages in exteriority, which increase valid interception area. So the results show that barrage net mode is suitable for the condition of enough pills.

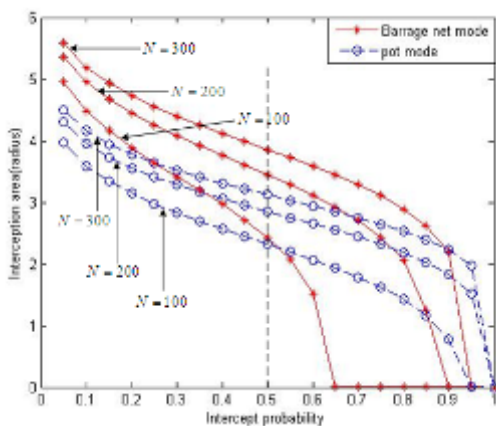


Fig 7. Relationship between interception area and intercept probability

From Fig.5-(2) with Fig.5-(3), we can see that when radius of barrage net increases, although its efficiency around pill configuration center is decreased, but valid interception area is increased, so barrage net mode is suitable for the condition of low forecasting precision for aerial flyer. When we adopt this shooting mode, size of barrage net can be adaptive set on the basis of forecasting error scope in order to assure optimal intercept probability.

Fig.6-(a) shows that within circular interception area of the same acreage, the smaller of pill distribution probability is correlated with the bigger radius of barrage net. When  $r = \sqrt{2}, \sigma = 1$ , its pill distribution probability is similar to that of point interception mode with the parameter  $\sigma = 2$ ; Fig. 6-(b) shows that when the looped area is near to pill configuration center, the smaller of its pill distribution probability is correlated with the bigger radius of barrage net. But when the looped area is far from pill configuration center, the bigger of its pill distribution probability is correlated with the bigger radius of barrage net. This means that the more of increasing valid interception area in periphery is correlated with the bigger radius of barrage net.

Fig.7 shows that when pill number is increased from 100 to 300, the max intercept probability of point mode will increase from 0.95 to 1.0, however that of barrage net mode will increase from 0.65 to 0.95, so the more obvious advantage of barrage net mode is correlated with more pills; If taking lower limit value of intercept probability as 0.5 (broken line in Fig.7 for instance), the valid interception area of Barrage net interception mode with  $N = 200$  is greater than that of point interception mode with  $N = 300$ . The results show that the self-design of point interception mode exists limitation, so this mode can not improve the valid interception area through increasing the number of pills.

Through dispersing excrescent pills from near pill configuration center to periphery, which will increase the valid intercept probability, barrage net interception mode can be used under condition of low forecasting precision of aerial flyer position. and when pills are enough, radius of barrage net can be reasonable set in order to assure optimal intercept probability; Point interception mode can assure the big intercept probability around pill configuration center, and can be used in the condition of little pill or high forecasting precision for aerial flyer.

### 5 Conclusions

In this paper, we propose two methods i.e., the point interception and barrage net interception, in order to intercept aerial flyer around security area effectively by using anti-aircraft gun system. The conception and principle of the two interception modes are defined, and the maneuverability for the latter mode is proved by probability theory. In fact, the relationships between the two methods are not mutually exclusive but complementary, because point interception mode is applied to the condition of high forecasting precision for aerial flyer position, and barrage net mode is applied to the condition with low precision, so the interception mode should be chosen on the basis of actual needs.

## Acknowledgement

This work is co-supported by Chinese NSFC under Grant 611410XX and the National Defense Technology Fund 40405070XX., Assistance from Wei Wang and Chuan-chuan Wang with the preparation of parts of this article is also appreciated. Finally, the authors would like to thank the anonymous reviewers for their valuable comments.

### References:

- [1] J. Crowder. Anti-Terrorism Learning Advisory System: Operative Information Software Agents (OISA) for *Intelligence Processing*. AIAA Infotech@Aerospace 2010 Online Proceeding, USA.
- [2] Zhong-xu WANG, Li CHEN. Implementation of Three Shooting Modes for Distributed Fire Control System of Antiaircraft Gun[J]. *Acta Armamentarii*, 2011, 32 (7): pp.795-800.
- [3] Zhong-xu WANG, Xue-biao ZHANG, An-dong SHENG. Research on fire control system based on distributed nodes[J]. *Acta Armamentarii*, 2005, 26(5):pp. 638-641.
- [4] Yu-ming BO, Zhi GUO, Guo-ping DU, et al. Complementation of archibald and antiaircraft missile in low range air and anti-missile defence[J]. *Acta Armamentarii*, 2002, 23(2): pp.164-166.
- [5] Jin-chun HU,Zhi GUO. Mathematical description of future airspace window[J]. *Acta Armamentarii*, 1998, 19(4): pp.293-297.
- [6] Jin-chun HU, Zhi GUO. On the optimisation of parameters for future airspace window[J]. *Acta Armamentarii*, 1999, 20(1): pp.13-18.
- [7] Shi-yan SUN, Zhi-ming QIU, WANG Hang-yu, et al. Dispersion Center Configuraion Method of Barrage Firing Curtain[J]. *Journal of Ballistics*, 2008, 20(4): pp.16-19.
- [8] Yuan-xing XIAO, Guan-jie ZHANG. Effectiveness Cost Analysis on Land-based Air Defense Weapon System[M] *Bei Jing:National Defense Industyr Press*, 2006,3.